

## $\alpha,\alpha$ -Trehalose/Water Solutions. 5. Hydration and Viscosity in Dilute and Semidilute Disaccharide Solutions

C. Branca, S. Magazù, G. Maisano, F. Migliardo, P. Migliardo,\* and G. Romeo

*Dipartimento di Fisica and INFM, Università di Messina, 98166 Messina, Italy*

*Received: January 17, 2001; In Final Form: April 26, 2001*

We report viscosity and compressibility measurements of trehalose, maltose, and sucrose aqueous solutions at different concentration and temperature values. What emerges from the concentration dependence of viscosity and compressibility is that trehalose, in comparison to maltose and sucrose, shows a higher interaction strength with water, which gives rise to a greater value of the hydration number throughout the investigated temperature range. Furthermore, viscosity measurements reveal that at high concentration values, trehalose shows a “stronger” kinetic character than the other disaccharides, namely, a lower structural sensitivity to temperature changes in the investigated temperature range. This result could explain the greater cryptobiotic attitude of trehalose at high concentrations. The present work, which consists of quantifying experimentally the basic hydration behavior and solution structure of the investigated disaccharides as a function of concentration and temperature, allows the working hypothesis of the several existing simulation approaches to be tested.

### I. Introduction

Trehalose is among the most chemically unreactive and stable sugars in nature. From a general point of view, trehalose ( $\alpha$ -D-glucopyranosil  $\alpha$ -D-glucopyranoside), maltose (4-O- $\alpha$ -D-glucopyranosil-D-glucose), and sucrose ( $\alpha$ -D-glucopyranosil  $\beta$ -D-fructofuranoside) have the same chemical formula ( $C_{12}H_{22}O_{11}$ , MW = 342.3) but different structures, which could account for the differences in the destructuring effectiveness.

Trehalose has been exploited for millenia by a range of desiccation-resistant organisms.<sup>1,2</sup> Empirical evidence shows that high concentrations of trehalose in the tissues of certain insects, yeasts, lactobacillus, mushrooms, and desert plants allow them to survive for decades, and in some cases centuries, in a state of suspended animation under conditions of water deficiency, resuming rapidly their active metabolism when rehydrated.<sup>3–6</sup> Furthermore, trehalose is used widely in nature also as a frost protectant, able to preserve living species from the damage caused by freezing.<sup>7</sup>

Green and Angell<sup>7,8</sup> suggest that the destructuring effectiveness of trehalose is related to its higher glass transition temperature. On the other hand, Crowe and co-workers<sup>9</sup> have noted that vitrification is not sufficient for preservation, and Crowe<sup>9,10</sup> proposed the water replacement hypothesis.

Therefore, a series of experimental studies have been performed, investigators focusing their attention on the molecular point of view. Raman scattering experiments<sup>11,12</sup> show that disaccharides obstruct the crystallization process, reducing the amount of freezable water, namely, destroying the network of water compatible with that of ice. In addition, it has been shown that, among the three disaccharides, trehalose promotes the most substantial *destructuring effect* on the tetrahedral H-bond network of pure water. Finally, a series of quasielastic neutron scattering (QENS) experiments<sup>13–15</sup> suggest that trehalose affects significantly the dynamics of water molecules in its environment consistently with the presence of a series of hydration layers or shells, each of which is characterized by a relatively slow diffusion. Such a result was confirmed by Brady and co-workers in a recent molecular dynamics (MD)<sup>16</sup> study. This slowing

effect has also been observed in aqueous mixtures of trehalose with sodium chloride. As noted by Conrad et al.,<sup>17</sup> the presence of ionic species influences considerably the dynamics of water in concentrated solutions. These systems are actually the subject of investigations since most biological systems of interest contain ionic solutes.<sup>18–20</sup> Finally, in a series of works reporting on the effects of embedding carbon-monooxy-myoglobin in trehalose glass on protein-specific motions, Cordone et al. suggest that trehalose coating prevents thermal denaturation by damping large-scale fluctuations of protein-specific motions.<sup>21</sup>

From the microscopic point of view, the interaction of trehalose with water has been investigated by three significant MD simulation studies.<sup>22–25</sup> The interaction of trehalose with water has been investigated, and results of statistical analyses on infinitely dilute aqueous solutions of trehalose have been reported. Bonanno et al.<sup>22</sup> have found that the total number of molecules within a 3.5 Å hydration shell at  $T = 27^\circ\text{C}$  is 35.9, 18.9 of which are hydrogen bonded to trehalose atoms. However, using more strict criteria for the hydrogen bond definition, that is, a distance between the proton and acceptor of  $<2.4$  Å and an angle formed by the donor, hydrogen, and acceptor of  $>145^\circ$ , they have found that the hydration number for the most diluted solutions (6 wt %) at  $27^\circ\text{C}$  decreases to 11.5, in reasonably good agreement with the value reported by Donnamaria et al.<sup>23</sup> The previous simulation did not handle long-range interactions in an exact or complete manner. The rigorous treatment of long-range interactions is important in the dynamic, structural, and thermodynamic properties of water and aqueous solutions.<sup>24</sup> Conrad et al.<sup>25</sup> paid special attention to the choice of model (force field) and treatment of long-range interactions, and their most interesting result is the confirmation of the presence of an intramolecular hydrogen bonding in trehalose at high concentration.

The main purpose of this work is to gain a better understanding of the hydration properties of aqueous solutions of homologous disaccharides and to compare the kinetic and thermodynamic “fragile” character. Therefore, we report viscosity and compressibility measurements of trehalose, maltose, and sucrose

aqueous solutions at different concentration and temperature values. What emerges from the concentration dependence of viscosity and compressibility is that a trehalose/water solution, in comparison with the maltose/ and sucrose/water solutions, shows a higher interaction strength with water at all the investigated temperatures. Furthermore, in comparison to the other homologous disaccharide/water solutions, the trehalose solution shows the strongest character at the investigated concentrations. Furthermore, the obtained findings fill the gap that exists in the literature concerning the hydration value data of these homologous disaccharides, allowing the reliability of the molecular simulation to be tested.<sup>22–25</sup>

## II. Experimental Section

The investigated samples were purchased from Aldrich-Chemie. The solutions were prepared by weight using double-distilled deionized water. Care was taken in order to obtain stable, clear, dust-free samples, and ample time was allowed for equilibration. In addition, the solutions were filtered with 0.45 μm Amicon filters and stored in the dark to minimize biological and photochemical degradation.

Viscosity measurements were performed in the temperature range of 20–85 °C by means of standard Ubbelohde viscometers on disaccharide aqueous solutions at different concentration values  $\phi$ , where  $\phi = n_d M_d / n_d M_d + n_w M_w$ , with  $n_d$  and  $M_d$  and  $n_w$  and  $M_w$  being the mole numbers and the molecular weights of the disaccharide and water, respectively. The viscometers were mounted in a suitable bath, which stabilized the temperature within  $\pm 0.02$  °C, and chosen with a long flow time in order to minimize the kinetic energy correction. Before the viscosity was measured, the samples were stabilized for a sufficient time at the given temperature. Experimental data turn out to be reproducible with an indeterminations lower than one part per thousand. Auxiliary density measurements, necessary to evaluate the shear viscosity of the solutions from the kinematic viscosity, were performed as a function of concentration and temperature using a standard picnometer technique.

Ultrasonic velocity measurements were performed on the three homologous disaccharide aqueous solutions at different concentration values by the pulse echo technique using a homemade acoustic interferometer working at the frequency of 3 MHz. We have checked, by performing measurements at various concentrations and for frequencies from 3 to 20 MHz, that the sound velocity is almost frequency-independent in this range, indicating that we are not observing possible relaxation processes. The electronic equipment consisted of a standard Matec, Inc., apparatus, and the measurements, performed using the echoes-overlapping method, were reproducible within 0.05%.

## III. Viscosity Data

As it is well-known, information on the hydration of solutes can be obtained by a procedure given by Linow and Philipp.<sup>26</sup> In a relatively simple geometric model based on Einstein's viscosity law,<sup>27</sup> a calculation of solvation numbers from the change of solution viscosity with solute concentration can be achieved. From eq 1, the value  $1/d = \bar{v}_\eta$ , the specific volume of the hydrated solute, can be obtained:

$$\frac{1}{d} = \eta_{\text{red}} \left( 1 + \frac{1}{f + \eta_{\text{sp}}} \right) \quad (1)$$

Here,  $f = 2.5$  and the expressions  $\eta_{\text{sp}} = (\eta - \eta_0)/\eta_0$  and  $\eta_{\text{red}} = \eta_{\text{sp}}/c$  are the specific and reduced viscosities, respectively, where the concentration  $c$  is measured in grams of solute per cubic

**TABLE 1: Density ( $\rho$ ) as a Function of Weight Fraction and Temperature (°C)**

$\rho_{\text{trehalose}} (\text{g}/\text{cm}^3)$					
$\phi$	$T = 20$	$T = 25$	$T = 40$	$T = 50$	$T = 60$
0.066	1.02456	1.02319	1.01816	1.01377	1.00880
0.160	1.06454	1.06319	1.05731	1.05249	1.04722
0.320	1.13950	1.13764	1.13151	1.12572	1.11993
0.500	1.22073	1.21985	1.21562	1.20880	1.20240
$\rho_{\text{maltose}} (\text{g}/\text{cm}^3)$					
$\phi$	$T = 20$	$T = 25$	$T = 40$	$T = 50$	$T = 60$
0.066	1.02435	1.02313	1.01785	1.01355	1.00860
0.160	1.06365	1.06235	1.05660	1.05201	1.04685
0.320	1.13801	1.13596	1.12901	1.12460	1.11860
0.500	1.22236	1.21994	1.21154	1.20702	1.20026
$\rho_{\text{sucrose}} (\text{g}/\text{cm}^3)$					
$\phi$	$T = 20$	$T = 25$	$T = 40$	$T = 50$	$T = 60$
0.066	1.02420	1.02287	1.01772	1.01340	1.00850
0.160	1.06352	1.06219	1.05651	1.05191	1.04680
0.320	1.13760	1.13596	1.12930	1.12450	1.11810
0.500	1.22177	1.21934	1.21213	1.20696	1.19948

centimeter of solution. It follows that the value of the specific volume does not depend on the numerical factor  $f$ ; thus, for the model used, the shape of the solute particles is not involved in the calculation of the hydration number.

On the other hand, from the solution density  $d$  (Table 1) and the water density  $d^\circ$ , the apparent specific volume of the solute<sup>28</sup> can be obtained:

$$v_\phi = \frac{1000(d^\circ - d)}{m d d^\circ M} + \frac{1}{d} \quad (2)$$

Here,  $m$  is the molality and  $M$  is the molecular weight of the solute.

The difference  $v_\eta - v_{2\phi}$  is the volume of the solvent bound per gram of solute, where  $v_{2\phi}$  is the apparent specific volume of the solute at an infinite dilution. Thus, all volume changes connected with the hydration process are included in the apparent specific volume of the solute. Hence, the hydration number  $n_h^\eta$ , i.e., the number of moles of bonded water molecules in the inner hydration sphere per mole of solute, is given by the extrapolation at an infinite dilution of the viscosity solute–solvent interaction strength parameter  $M'$  defined by

$$M' = \frac{\rho(\bar{v}_\eta - \bar{v}_{2\phi})M_w}{M_d} \quad (3)$$

where  $M_d$  and  $M_w$  are molecular weights of the solute and solvent, respectively.

$$n_h^\eta = \lim_{c \rightarrow 0} M' \quad (4)$$

The concentration behavior of  $M'$  for the three disaccharides at  $T = 25$  °C is shown in Figure 1. It emerges that, in comparison to the water systems of the other disaccharides, the trehalose/water system is characterized by the highest value of  $M'$  throughout the investigated concentration range'. The fact that trehalose is more strongly hydrated than sucrose was already anticipated by Ekdawi and de Pablo.<sup>29</sup> These authors present hydration numbers for both sucrose and trehalose as a function of concentration, and the experimental data reported here confirm these predictions.

By extrapolating at an infinite dilution of the  $M'$  values, we have evaluated the hydration numbers  $n_h^\eta$ . They are reported as

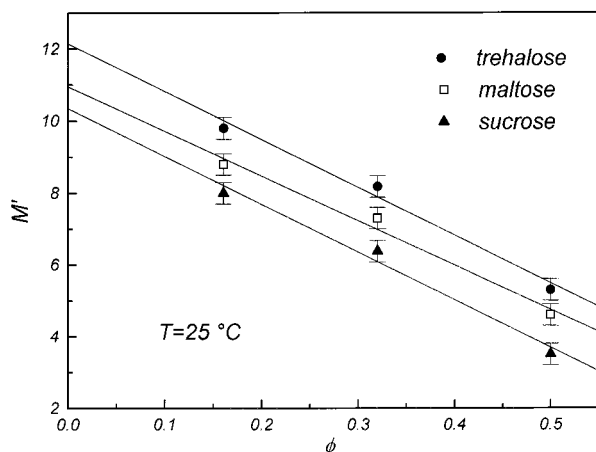


**Figure 1.** Concentration behavior of  $M'$  for the three disaccharides at  $T = 25\text{ }^{\circ}\text{C}$ .

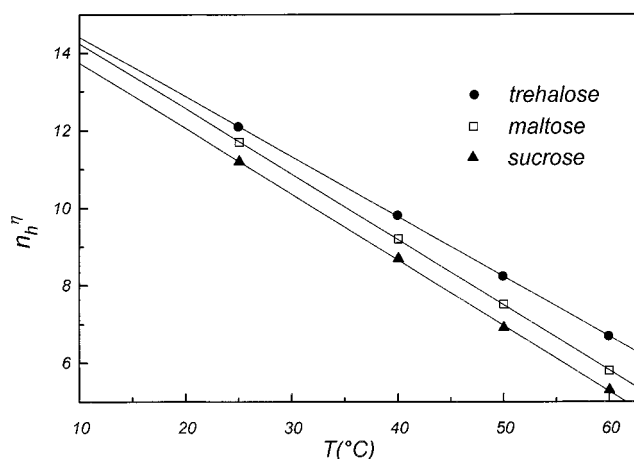


**Figure 2.** Temperature behavior of the hydration number for the three disaccharides.

a function of temperature in Figure 2. It can be seen that  $n_h^{\eta}$  decreases with increasing temperature as a result of different effects. In fact, it is expected that increasing the temperature will decrease the average number of water molecules moving together with sugar due to the enhanced thermal motions. At the same time, it should also be pointed out that with increases in temperature, owing to the rupture of a certain fraction of hydrogen bonds in water, the number of water molecules available for bonding with the solute increases too. Finally, the excluded volume interactions for increasing values of temperature increase and tend to swell the solute structure. Therefore, the observed behavior is determined by the net result of these three effects. Far more important, we can observe from Figure 2 that, in comparison to the other disaccharide solutions, the trehalose/water system is characterized by the highest value of hydration number in the entire temperature range.

As it is well-known, we can also obtain information about the fragility degree of a liquid from viscosity measurements. The classification of liquids as having different degrees of “strong” and “fragile” behavior<sup>8,30,31</sup> is an increasingly important matter as a framework for describing relaxation in liquids. In terms of the Angell’s classification,<sup>32</sup> glass-forming materials are regarded in a strong limit viscosity, obeying the Arrhenius law given by

$$\eta \propto \exp(E/K_B T) \quad (5)$$

The other limit is, on the other hand, called fragile glass, where

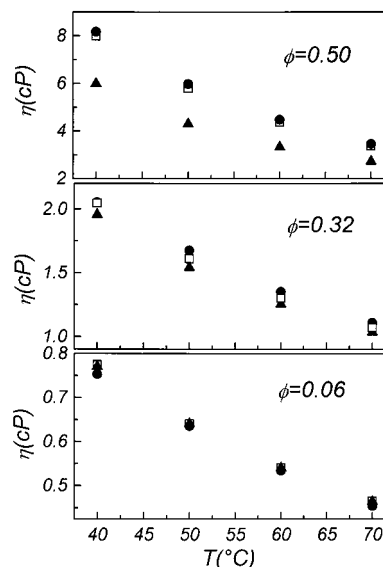


**Figure 3.** Shear viscosity as a function of temperature at different weight fractions ( $\phi = 0.06, 0.32$ , and  $0.50$ ).

viscosity obeys the highly non-Arrhenius Vogel–Tamman–Fulcher<sup>33</sup> function (VTF):

$$\eta \propto \exp\left[\frac{DT_0}{(T - T_0)}\right] \quad (6)$$

The parameter  $D$ , named the *strength parameter*, controls how closely the system obeys the Arrhenius law ( $D \rightarrow \infty$ ). As  $D$  changes, so will the value of  $T_0$  relative to the glass transition temperature  $T_g$ , the scaling temperature at which the viscosity value is equal to  $10^{13}$  P. From these considerations, one finds that  $D$  is connected with  $T_0$  and  $T_g$  by<sup>33</sup>

$$\frac{T_g}{T_0} = 1 + \frac{D}{2.303 \log(\eta_g/\eta_0)} \quad (7)$$

with  $\log(\eta_g/\eta_0) \cong 17$ .

One of the most useful aspects is the fact that in order to investigate the fragile character of a system, it is not necessary to perform measurements down the glass transition temperature. In fact, by knowing the temperature dependence of viscosity, one can obtain information on the thermal sensitivity, namely, the resistance of the configurational short- and medium-range order to thermal degradation of the system near  $T_g$ . Throughout the temperature range, until the glass transition is reached, fragile systems are characterized by an increasing activation energy value as the temperature is lowered toward  $T_g$ . This corresponds to a strongly non-Arrhenius behavior.

Figure 3 displays the shear viscosity of the three disaccharides as a function of temperature at different weight fractions of  $\phi = 0.06, 0.32$ , and  $0.50$ . Although the temperature dependence appears to be similar for the three disaccharides, data differ, in a more marked way, at the lowest temperatures and especially at the highest concentration value. At this concentration value, in fact, as shown in Figure 3, the trehalose/water system shows a lower structural sensitivity to temperature changes in comparison to the other disaccharide solutions. As it is well-known, this behavior has been ascribed to the fragility degree of a glass-forming liquid. Following Adam and Gibb’s picture,<sup>30</sup> it is well-known that the complexity of the  $(3N + 1)$ -dimensional potential-energy hypersurface in the configuration space explored by the system can be connected with the density of

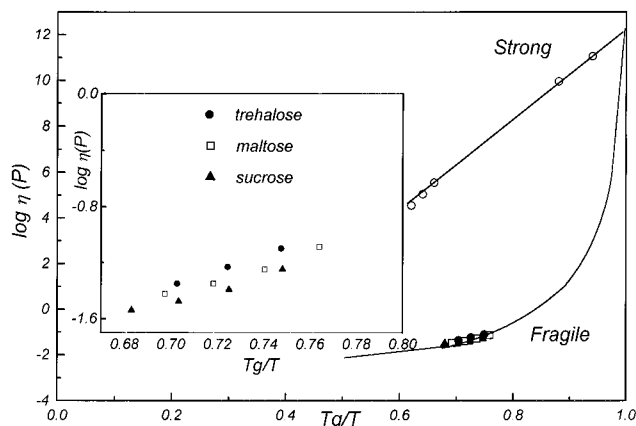


**Figure 4.** Scaled Arrhenius representation of viscosity data of trehalose (solid circles)/, maltose (open squares)/, and sucrose (solid triangles)/water solutions at  $\phi = 0.50$ .  $\text{SiO}_2$  data (open circles) are provided for comparison. The straight lines are the fit result according to the VTF equation. A magnification is shown in the inset.

minima of the hypersurface (degeneracy) and with the distribution of the barrier heights between them. The fragility parameter  $\chi$  can be connected with the ratio between the density of minima of the potential-energy hypersurface in the configurational space ( $\propto \Delta C_p(T_g)$ ) and the barrier heights  $\Delta\mu$  between them or, equivalently, to the shear viscosity  $\eta$ <sup>34–37</sup>

$$\chi = \Delta C_p(T_g)/\Delta\mu = \frac{d \log \eta}{d(T_g/T)} \bigg|_{T=T_g} \quad (8)$$

In the previous relation,  $\chi_{\min} \cong 16$  is within the limit of a strong system.

Knowing the glass transition temperatures of the three disaccharide glass formings at  $\phi = 0.50$  ( $T_g \cong -40$  °C for sucrose,  $T_g \cong -39$  °C for maltose, and  $T_g \cong -35$  °C for trehalose at the fixed concentration), to highlight their different rigidities, we have reported (see Figure 4) our viscosity data in an Angell plot together with the viscosity values from the literature<sup>38</sup> of  $\text{SiO}_2$ , a conventional strong system. The straight lines represent the fit result according to eq 6. In the inset, a magnification relative to the disaccharide solution data is reported. Following the procedure cited above, we have evaluated the fragility parameter value  $\chi$  from the fit parameters. For the trehalose solution at  $\phi = 0.50$ , one finds that  $\chi = 107.4$ , while for the sucrose and maltose solutions at the same concentration,  $\chi = 111.0$  and  $109.5$ , respectively. These values indicate that, in comparison to the other disaccharide/water systems, the trehalose/water system shows the strongest character. This finding is in good agreement with DSC measurements.<sup>39</sup> In fact, it has been reported that at a concentration value of  $\phi = 0.50$ , trehalose shows a much more marked glass transition than sucrose and maltose ( $\Delta C_p \approx 0.07 \text{ J g}^{-1} \text{ K}^{-1}$ ) in comparison with the sucrose mixture ( $\Delta C_p \approx 0.09 \text{ J g}^{-1} \text{ K}^{-1}$ ), indicative of a stronger character. Calorimetric solution properties of many disaccharides have also been extensively studied, and an interpretation of the heat of solution of the amorphous disaccharides in terms of their capacity to hydrogen bond to water has been provided. According to this study, hydrogen bonding in trehalose is more pronounced than in other disaccharides.<sup>40</sup>

#### IV. Acoustic Data

A comparison of the different hydration properties of the three homologous disaccharide/water solutions has also been carried

**TABLE 2: Acoustic Velocity Data ( $v_s$ ) as a Function of Weight Fraction at  $T = 25$  °C**

$\phi$	trehalose $v_s$ (m/s)	maltose $v_s$ (m/s)	sucrose $v_s$ (m/s)
0.066	1486.9	1477.85	1478.1
0.160	1545.6	1450.81	1450.9
0.320	1645.2	1403.6	1403.9
0.500	1749.6	1353.2	1354.8

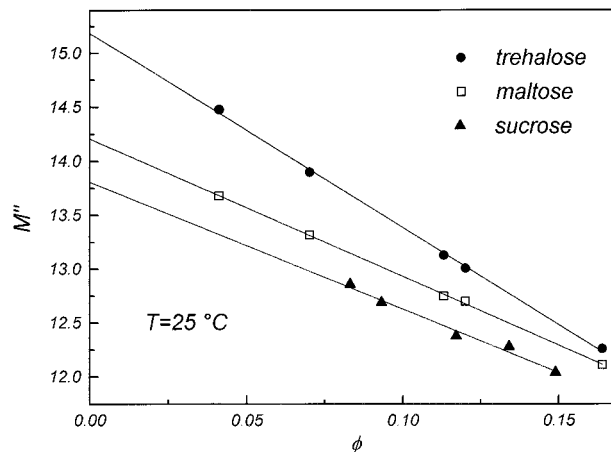


**Figure 5.** Compressibility solute-solvent interaction strength parameter  $M''$  of the three disaccharide/water solutions as a function of concentration. The continuous lines represent the result of a polynomial fitting procedure.

out by performing ultrasonic velocity measurements on trehalose, maltose, and sucrose aqueous solutions as a function of concentration and temperature (Table 2). Through an evaluation of the adiabatic compressibility coefficient using the Lorentz relationship  $\beta = 1/\rho v^2$ , we are able to get information on the disaccharide hydration number  $n_H$ . In fact, following a molecular model,<sup>41</sup> we assume that the volume of the solution  $V$  can be partitioned into two contributions: the hydration volume  $V_H$ , where significant interactions between the disaccharide and water occur, and the bulk water volume  $V_w$ . Following this model, we can express the volume of the solution as  $V = n_d V_H + (n_w - n_d n_H) V_w$ , where  $n_d$  and  $n_w$  are the mole numbers of the disaccharide and water, respectively. On the basis of the hypothesis of negligible compressibility for hydrated units, we can obtain the solute-solvent interaction strength as  $M'' = (n_w/n_d) (1 - \beta/\beta_w)$ , where  $\beta$  and  $\beta_w$  are the adiabatic compressibilities of the solution and water, respectively. From the extrapolation at an infinite dilution of the compressibility solute-solvent interaction strength parameter, we can evaluate the hydration number:

$$n_h^\beta = \lim_{n_d \rightarrow 0} M'' \quad (9)$$

In Figure 5, as an example, the behavior of  $M''$  as a function of concentration is reported for trehalose, maltose, and sucrose solutions at  $T = 25$  °C. The continuous lines represent the result of a polynomial fitting procedure.

It clearly emerges that, in comparison to the other disaccharide solutions, the trehalose/water system is characterized, throughout the investigated concentration range, by both the highest value of interaction strength and, as a consequence, the highest value of hydration number. For example, at  $T = 25$  °C,  $n_h^\beta = 15.2$  for trehalose,  $n_h^\beta = 14.7$  for maltose, and  $n_h^\beta = 14.1$  for sucrose. The agreement of our data with those reported by other authors is fairly good.<sup>28</sup> The experimental data reported here are in good



**TABLE 3: Hydration Number Deduced by Acoustic and Viscosity Data at  $T = 25\text{ }^{\circ}\text{C}$** 

	acoustic data, $n_h^{\beta}$	viscosity data, $n_h^{\eta}$
trehalose	15.2	12.1
maltose	14.2	11.7
sucrose	13.8	11.2

agreement with the predictions of Conrad and De Pablo and of Ekdawi-Sever et al.<sup>25,29</sup> Using a fully flexible SPC/E/water model, these authors have found that the hydration number of trehalose, the average number of waters hydrogen bonded per trehalose molecule over the course of the simulation, decreases monotonically from 12.8 at 6 wt % to 3.2 at 90 wt % at 85  $^{\circ}\text{C}$  and from 13.4 to 3.4 for the same range at 25  $^{\circ}\text{C}$ .

The observed behavior confirms the existence of a stronger and more complex interaction mechanism for the trehalose/water system, which is also responsible for the greater destructuring effect on the H-bond tetrahedral network of pure water. Furthermore, as we can see from Table 3, the obtained data are in good agreement with the  $n_h^{\eta}$  findings obtained by viscosity measurements.

It is well-known that the main drawback in calculating hydration numbers from ultrasonic measurements is the assumption that the compressibility of trehalose with its closely associated water molecules is negligible.<sup>41</sup> Inherent in this model is the further assumption that the compressibility of water molecules near, but not inside, the primary hydration shells is the same as that of pure water. Therefore, in general, the hydration numbers derived in this way can be different from those derived by means of *local* probes such as neutron scattering or EXAFS; they can also differ because of differences in the models used with the various approaches and critical assumptions underlying these models. In particular, at high concentration values, apart from simple interactions between water and trehalose, other interactions could come into play, and as a consequence, the compressibility behavior could be related to the structural arrangement of the whole system rather than that of specific entities. However, in our case, despite the simplicity of the model, due to the highly diluted concentration range investigated, which allows the neglect of solute–solute interactions, the values obtained for the hydration numbers are in good agreement with those calculated at room temperature by means of recent MD simulation studies.<sup>24,25</sup> The apparent discrepancy in the experimental determination of the hydration number is intriguing and points toward a different definition of hydration number.

## V. Conclusions

There is no doubt that to understand the molecular mechanisms determining the destructuring effectiveness of trehalose, it is important to characterize the structural and dynamics properties of disaccharide/water solutions over a wide temperature range and compare experimental data to the available simulation results.

The present work quantifies experimentally the basic hydration behavior and solution structure of the three disaccharides as a function of concentration and temperature. We have reported some experimental findings obtained by density, viscosity, and sound velocity measurements on trehalose, maltose, and sucrose aqueous solution.

Viscosity and ultrasonic data reveal that, in comparison to the other disaccharide solutions, the trehalose/water system is characterized by the highest values of the interaction strength

parameter of the hydration number. Most interesting of these results is the good agreement of the hydration number values obtained by ultrasonic and viscosity measurements with those obtained by MD simulations.

The greater interaction strength can justify the greater destructuring effectiveness of trehalose on the tetrahedral hydrogen bond network of water. Such a destructuring effect, which inhibits water molecules from assuming positions and orientations compatible with the formation of ice, could explain the exceptional cryoprotecting properties of trehalose in comparison to those of the other disaccharides.

Finally, viscosity findings also support the hypothesis of a more highly strong thermodynamic character of the trehalose/water system at low water content in comparison to those of the other disaccharides. Further investigations are actually in progress to elucidate the interaction mechanisms underlying the bioprotective properties of trehalose and to get more insight into the thermophysical properties of disaccharide aqueous solutions.

## References and Notes

- (1) Crowe, J. H.; Crowe, L. M. In *Biological Membranes*; Chapman, D., Ed.; Academic Press: New York, 1984; p 57.
- (2) Elbein, A. D. *Chem. Biochem.* **1974**, *30*, 227.
- (3) Vegis, A. *Annu. Rev. Plant Physiol.* **1964**, *15*, 185.
- (4) Sussman, A. S.; Halvorson, H. O. *Spores: Their Dormancy and Germination*; Harper & Row: New York, 1966.
- (5) Clegg, J. S. *Comput. Biochem. Physiol.* **1967**, *20*, 8.
- (6) Colaco, C.; Sen, S.; Thangavelu, M.; Pinder, S.; Roser, B. *Bio/Technology* **1992**, *10*, 1007.
- (7) Green, J. L.; Angell, C. A. *J. Phys. Chem.* **1989**, *93*, 2880.
- (8) Angell, C. A. *NATO-ASI Ser. B* **1991**, *329*, 59.
- (9) Crowe, J. H.; Leslie, S. B.; Crowe, L. M. *Cryobiology* **1994**, *31*, 355.
- (10) Crowe, J. H.; Carpenter, J. F.; Crowe, L. M. *Annu. Rev. Physiol.* **1998**, *60*, 73.
- (11) Branca, C.; Magazù, S.; Maisano, G.; Migliardo, P. *J. Phys. Chem. B* **1999**, *103*, 1347.
- (12) Branca, C.; Magazù, S.; Maisano, G.; Migliardo, P. *J. Chem. Phys.* **1999**, *111*, 281.
- (13) Magazù, S.; Majolino, D.; Middendorf, H. D.; Migliardo, P.; Musolino, A. M.; Sciortino, M. T.; Wanderlingh, U. In *Biological Macromolecular Dynamics*; Cusack, S., Ed.; Adenine: New York, 1996; p 155.
- (14) Magazù, S.; Maisano, G.; Majolino, D.; Migliardo, P.; Musolino, A. M.; Villari, V. *Prog. Theor. Phys.* **1997**, *126*, 195.
- (15) Magazù, S.; Villari, V.; Migliardo, P.; Maisano, G.; Telling, M. T. *F. J. Phys. Chem. B* **2001**, *105*, 1851–1855.
- (16) Liu, Q.; Schmidt, R. K.; Teo, B.; Karplus, P. A.; Brady, J. W. *J. Am. Chem. Soc.* **1977**, *99*, 785.
- (17) Miller, D. P.; Conrad, P. B.; Fucito, S.; Corti, H. R.; de Pablo, J. J. *J. Phys. Chem. B* **2000**, *104*, 10419–10425.
- (18) Miller, D. P.; de Pablo, J. J. *J. Chem. Phys.* **1996**, *104*, 664.
- (19) Miller, D. P.; de Pablo, J. J.; Corti, H. R. *J. Pharm. Res.* **1997**, *14*, 578.
- (20) Miller, D. P.; de Pablo, J. J.; Corti, H. R.; et al. *J. Phys. Chem. B* **1999**, *103*, 10243–10249.
- (21) Cordone, L.; Galajda, P.; Vitranò, E.; Gassmann, A.; Ostermann, A.; Parak, F. *Eur. Biophys. Lett.* **1998**, *27*, 173 and references therein.
- (22) Bonanno, G.; Noto, R.; Fornili, S. L. *J. Chem. Soc., Faraday Trans.* **1998**, *94*, 2755–2762.
- (23) Donnamaria, M. C.; Howard, E. I.; Grigera, J. R. *J. Chem. Soc., Faraday Trans.* **1994**, *90*, 2731–2735.
- (24) Conrad, P. B.; de Pablo, J. J. *Fluid Phase Equilib.* **1998**, *150*–151, 51–61.
- (25) Conrad, P. B.; de Pablo, J. J. *J. Phys. Chem. A* **1999**, *103*, 4049–4055.
- (26) Linow, K. J.; Philipp, B. *Z. Phys. Chem.* **1984**, *265*, 321–329.
- (27) Seymour, R. B.; Carraher, C. E., Jr. In *Polymer Chemistry. An Introduction*; Lagowski, J., Ed.; Marcel Dekker: New York, 1998; pp 432, 439–441.
- (28) Galema, S.; Hoiland, H. *J. Phys. Chem.* **1991**, *95*, 5321–5326.
- (29) Ekdawi-Sever, N. C.; Conrad, P. B.; de Pablo, J. J. *J. Phys. Chem. A* **2001**, *105*, 734–742.
- (30) Angell, C. A. *J. Phys. Chem. Solids* **1988**, *49*, 863.
- (31) Angell, C. A. *J. Non-Cryst. Solids* **1991**, *13*, 131–133.

- (32) Angell, C. A. *Science* **1995**, 267, 1924–1933.
- (33) Vogel, H. Z. *Phys.* **1921**, 22, 645.
- (34) Wang, G. M.; Haymet, A. D. J. *J. Phys. Chem. B* **1998**, 102, 5341–5347.
- (35) Bohmer, R.; Angell, C. A. *Phys. Rev. B* **1992**, 45, 10091.
- (36) Roos, Y.; Karel, M. *Cryo-Lett.* **1991**, 12, 367–376.
- (37) Stuher, J.; Yeager, E. In *Physical Acoustic*; Mason, P. W., Ed.; Academic Press: New York, 1965; p 351.
- (38) Angell, C. A.; Bressel, R. D.; Green, J. L.; Kanno, H.; Oguni, M.; Sare, E. J. *J. Food Eng.* **1994**, 22, 115–142.
- (39) Wang, G. M.; Haymet, A. D. J. *J. Phys. Chem. B* **1998**, 102, 5341–5347.
- (40) Miller, D. P.; de Pablo, J. J. *J. Phys. Chem. B* **2000**, 104, 8876–8883.
- (41) Stuher, J.; Yeager, E. In *Physical Acoustic*; Mason, P. W., Ed.; Academic Press: New York, 1965; p 351.